# 2D indoor localization system using FMCW radars and DMTD technique

**Conference Paper** · October 2014

DOI: 10.1109/RADAR.2014.7060365

CITATIONS
2

READS
496

**3 authors:**

Rupesh Kumar
XLIM Research Institute
**17** PUBLICATIONS **12** CITATIONS
SEE PROFILE

Jean-christophe Cousin
Télécom ParisTech
**41** PUBLICATIONS **114** CITATIONS
SEE PROFILE

Bernard Huyart
Institut Mines-Télécom
**186** PUBLICATIONS **917** CITATIONS
SEE PROFILE

# 2D Indoor Localization System Using FMCW Radars and DMTD Technique

Rupesh Kumar, Jean-christophe Cousin, Bernard Huyart
Institute Mines-Telecom, Telecom ParisTech - LTCI CNRS UMR 5141
46 rue Barrault 75634 Paris cedex 13, France
rupesh.kumar@telecom-paristech.fr

***Abstract*—A multistatic microwave frequency-modulated continuous-wave (FMCW) radar system used to localize a remote Tag in an Indoor Environment is described. The frequency information extracted from the FMCW data can be processed for the range and the angle-of-arrival (AoA) estimation by computing the average frequency shift over a fixed sweeping period of time by utilizing the DMTD (Dual Mixer Time Difference) technique. This allows one to reduce the sweeping frequency range while maintaining the accuracy.**

***Keywords— Indoor Localization; FMCW Radar ; range; angle-of-arrival; DMTD;***

## I. INTRODUCTION

The indoor localization of people is a real challenge in terms of accuracy. In this case, the GPS solution doesn't satisfy because of the strong attenuation of signals and the multipath effects. Many solutions are proposed as the trilateration based on the RSSI measurement [1]; the main advantage is the availability of the existing WLAN networks, for example WiFi-network. In this case, at least 3 base stations are required to help a mobile to localise itself. The main drawback is the requirement of the prior knowledge about the indoor propagation channel which is a compulsory condition for obtaining a localization error in meters while utilizing the fingerprinting method [2]. Another way to obtain an indoor localization is to measure the Time-of-Flight (TOF) of the wave between radar and target/mobile supposed to be localized. Some solutions proposed as the use of FMCW Radar systems [3-5] for better performance. The FMCW technique enables the measurement of the frequency difference between a transmitted reference signal and echo (coming from the searched target as a reflected wave). This frequency difference is carried out by the baseband sinusoidal signal which is obtained by mixing the reference signal with the incoming signal as an echo from the intended target. This obtained frequency shift is a function of the distance between the radar and the target. In most of cases, the measurements consist of the FFT processing for obtaining the frequency shift. This step may be time consuming if an accurate value of this frequency is required with high sampling frequency. Another method to measure the frequency difference is to integrate the continuous phase shift of the obtained sinusoidal signal over a known fixed duration time. This interferometeric method allows the detection of the distance [5]. Further, this phase shift information can be used to compute the range and the AoA as mentioned in [5]. If the range measurement is easily obtained as mentioned before, the AoA measurement needs a multistatic radar structure [5]. In that case, the AoA is calculated from the comparison of the different baseband signals. To compute the measured range and AoA, the Dual-Mixer Time Difference (DMTD) method may be used [5].

This paper describes a way to calculate the interferometeric phase-shift information, which can be implemented on a multistatic FMCW Radar system for 2D measurement as presented in [5]. Further, the effects of the system's frequency bandwidth has been analysed on 2D measurement in a real indoor environment while considering Line-of-Sight (LOS) case.

The paper has been organised as follow: Section II presents the DMDT method for range and angle computations. The comparison between the known values and estimated ones are presented and discussed in Section III for different values of the system's frequency bandwidth. Finally, the conclusion is drawn in Section IV.

## II. THEORY

The DMTD method is described in this part. It is based on the time delay measurement as presented in Fig.1

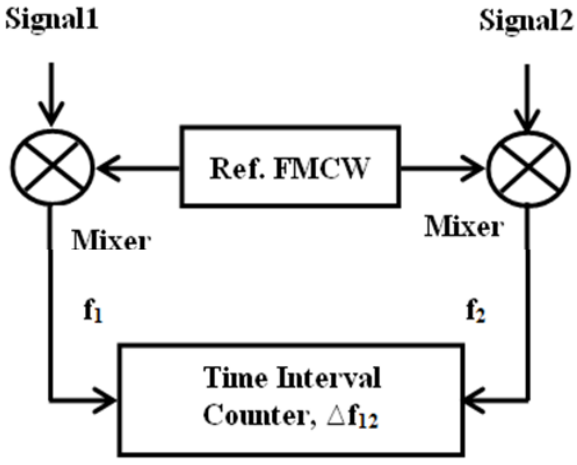


Fig. 1. DMTD- time delay measurement scheme.

Assuming that Signal1 and Signal2 are provided from echoes of the Ref FMCW signal and travelling different paths,

these two signals are mixed with the Ref. FMCW covering the [6-7GHz] frequency bandwidth. At the output of each mixer, $f_1$ & $f_2$ are the beat frequencies of the obtained sinusoidal signals after the down conversion of the two incoming signals, Signal1 & Signal2 with respect to the Ref FMCW signal. The difference between $f_1$ & $f_2$, denoted as $\Delta f_{12,}$ is computed by the Time Interval counter and is given by the expression:

$$f_2 - f_1 = \Delta f_{21} \tag{1}$$

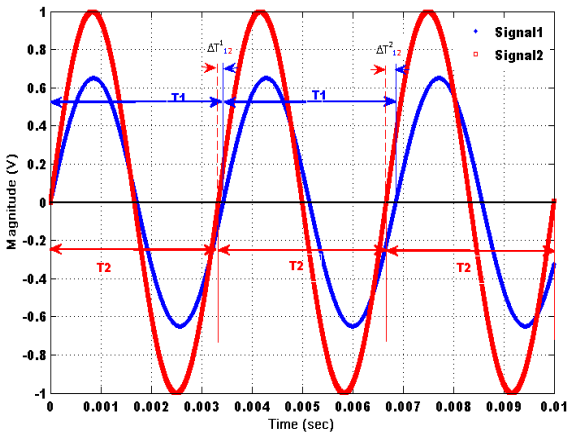


Fig. 2. Simulated Signal1 and Signal2.

The time periods corresponding to $f_1$ & $f_2$ are given by,

$$T_1 = 1/f_1 \quad T_2 = 1/f_2 \tag{2}$$

The difference in time period can be expressed as

$$\Delta T = T_1 - T_2 = \Delta T_{12}^{2nd} - \Delta T_{12}^{1st} = \ldots = \Delta T_{12}^{N} - \Delta T_{12}^{N-1} \tag{3}$$

Where, $\Delta T^{N\text{-}th}{}_{12}$ is the $N^{th}$ time period difference between the $N^{th}$ cycle of $f_1$ & $f_2$, respectively, and $\Delta T$ is the constant successive difference between two consecutive cycles, see Fig 2.

Thus, the average value of the N cycles can be written as

$$\frac{\sum_{i=1}^{N} \Delta T^i}{N} = \frac{\left(\Delta T_{12}^{2nd} - \Delta T_{12}^{1st}\right) + \ldots + \left(\Delta T_{12}^{N} - \Delta T_{12}^{N-1}\right)}{N} \tag{4}$$

Also, the average time period for the two signals for N number of cycles can be written as

$$\frac{\sum_{i=1}^{N} T_1^i}{N} = \frac{T_1^{1st} + T_1^{2nd} \ldots + T_1^{N-th}}{N} \tag{5}$$

$$\frac{\sum_{i=1}^{N} T_2^i}{N} = \frac{T_2^{1st} + T_2^{2nd} \ldots T_2^{N-th}}{N} \tag{6}$$

Now, $\Delta f_{21}$ can be expressed in terms of $T_1$ & $T_2$ as

$$\Delta f_{21} = \frac{1}{T_2\left(1 + T_2/\Delta T\right)}$$

Where, $\Delta T$ is given by (3).

The above expression can be generalized for N, the number of cycles, as

$$\frac{\sum_{i=1}^{N} f_{21}^i}{N} = \frac{1}{\frac{\sum_{i=1}^{N} T_2^i}{N}\left(1 + \frac{\frac{\sum_{i=1}^{N} T_2^i}{N}}{\frac{\sum_{i=1}^{N} \Delta T^i}{N}}\right)}$$

$$= \frac{1}{\frac{\sum_{i=1}^{N} T_2^i}{N}\left(1 + \frac{\sum_{i=1}^{N} T_2^i}{\sum_{i=1}^{N} \Delta T^i}\right)} \tag{7}$$

Therefore, the average value of the frequency difference for N cycles between Signal1 & Signal2 is expressed by (7). So the frequency difference between the Signal1 & Signal2 can help in the path-difference calculation with the FMCW Radar equation [5] and the relationship (7) as,

$$Path\_dif = \left(\Delta f_{21} * T_m * c\right)/BW \tag{8}$$

Where Tm is the FMCW signal's sweep-time $T_m$, c is the speed of light, and BW is the frequency bandwidth.

Further, The AoA can be computed from (8) by the relation mentioned in [5] as

$$\alpha = \cos^{-1} \frac{Path\_dif}{d_{baseline}} \tag{9}$$

With $d_{baseline}$ is the distance between the two receiver antennas. The range/radial distance can be computed with (5) & (6) as presented in [5],

$$d_i = \left(0.5 * f_i * T_m * c\right)/BW$$

$$= \left(0.5 * T_m * c\right)/\left(T_i * BW\right) \tag{10}$$

Where, 'i' is either 1 or 2.

Thus, the DMTD method can be used for the 2D measurement by evaluating the frequency-shift.

## III. MEASUREMENTS AND RESULTS

The estimation of the range and angle-of-arrival in a real indoor environment for a LOS case is presented in this section. To estimate the influence of the frequency bandwidth, we compare the results using frequency bandwidth of 1 GHz and 500 MHz, respectively. The position of the remote active-Tag to localize is estimated in polar form, i.e. range and angle with respect to the known position of Localization Base Station (LBS).

The section-A shows the system setup for the localization and the system calibration is presented in the section B. The implementation of the theoretical relationships (1-10) is mentioned in section-C and finally, the results related to the estimated parameters are explained in section-D.

### *A. Measurement Set-up*

The measurement setup consists of two parts, LBS and active-Tag, which are shown in Fig 3.

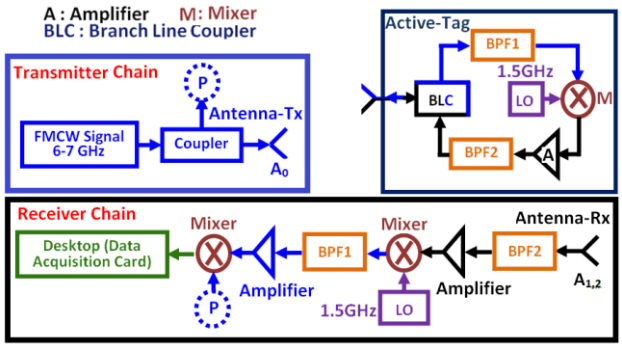


Fig. 3. Architecture defined for the LBS & active Tag

The LBS contains one Transmitter chain and two Receiver chains. The transmitting antenna [7] ($A_0$) and two receiving antennas ($A_1$ & $A_2$) [7] are placed on the same axis as shown in Fig 4. The transmitted signal is a linearly swept FMCW signal (used bandwidths are mentioned in Table I) with a sweep time, $T_m$=10 msec. It is transmitted from $A_0$ and received & sent back by the remote active-Tag [8]. The received signal at the LBS reaches the $A_1$ & $A_2$ antennas with a delay of $T_{Delay1}$ & $T_{Delay2}$, respectively. The received signals are down-converted to the baseband signal by super-heterodyne receivers. Firstly the signals received by $A_1$ and $A_2$ are filtered by BPF2( bandpass filter) and down converted by 1.5GHz. The baseband signals are obtained by mixing the down converted signals with the reference FMCW signal. The baseband signals carry the information about the frequency shift. The range estimation is performed using (10) and the AoA (α) computation is given from (9) as mentioned in [5].

The tag is used as an active one and its main application is to shift the incoming signal's frequency from $A_0$ by 1.5 GHz with the up converter mixer M (see Fig 3) and to retransmit it towards the LBS. In the active-Tag, two band pass filters (BPF1 & BPF2, see Table I) are used to avoid the feedback effects. The frequency shift of 1.5GHz also helps in reducing the coupling effects among the LBS's antennas ($A_0$ & $A_1$-$A_2$) and the back-scattering effects of the indoor propagation channel.

The above setup has been used for two different frequency bandwidths in order to investigate the effects on the accuracy. The signal set-up for the two cases is mentioned in Table I.

TABLE I. SIGNAL SET UP

| Setup | Bandwidth | BPF1 | BPF2 | FMCW Signal |
|---|---|---|---|---|
| 1 | 1 GHz | [6-7]GHz | [7.5-8.5]GHz | [6-7]GHz |
| 2 | 500 MHz | [6.5-7]GHz | [8-8.5]GHz | [6.5-7]GHz |

### *B. Calibration of the system*

In order to validate the measurement setup, the delays in system's circuit (transmitter, Tag & receivers) must be estimated. The configuration used for the calibration is depicted in Fig 4.

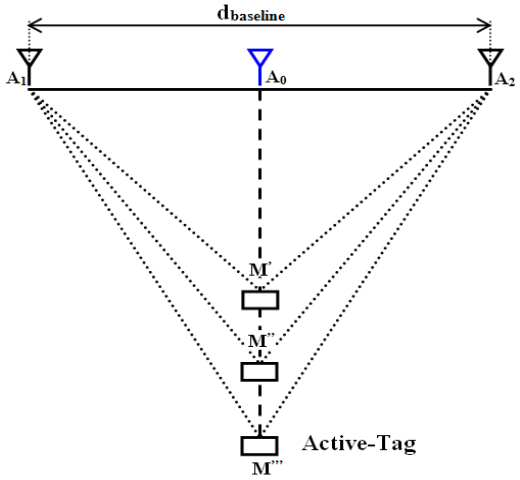


Fig. 4. Scheme for system calibration

The transmitter antenna ($A_0$) is kept at the midpoint of baseline ($d_{baseline}$) and the two receiver antennas ($A_1$ & $A_2$) are placed at the each end of the baseline. The active-Tag is placed on an orthogonal axis crossing the baseline at $A_0$.

The calibration is performed for the fixed length of baseline, i.e. $d_{baseline}$=0.30m. The active-Tag is placed on different points on the $A_0$-M``` axis. Hence, the distance measured from the receiver chains linked to the $A_1$ & $A_2$ antennas must be the same. Also, the angle-of-arrival (AoA) measured by the receiver antennas must always remain the same, i.e. 90°, with respect to the baseline.

The distance (between LBS and active-Tag) covers the (0. 9-1.5m) range. In TABLE II, the both setups (FMCW signals and used frequency bandwidths) and the observed distances unbalances are reported. The unbalances present the measured difference of paths between the transmitter and the receivers' chains Rx1 and Rx2 for the two considered frequency bandwidths.

TABLE II. ESTIMATED DELAYS FOR CALIBTRATION

| Setup | Bandwidth | distances unbalances | Tx FMCW Signal |
|---|---|---|---|
| 1 | 1 GHz | 1 cm | [6-7]GHz |
| 2 | 500 MHz | 4 cm | [6.5-7]GHz |

These unbalances are given for a range upto 1.5m. It accounts the round trip delays of the waves between the LBS and the active-Tag and including the delays inside the LBS (including the transmitter chain and the two receiver chains) and the active-Tag. Therefore, the range estimation can be written as

$$d_{fi} = d_i - dc_i \tag{11}$$

Where, $dc_i$ is obtained by the calibration, and i=1,2, '$d_i$' are the distances obtained by the relationship 10 and '$dc_i$' is the delay computed by the calibration and '$d_{fi}$' represents the estimated value, respectively.

### C. Range and Angle-of-Arrival estimation

The general description for the range and angle (AoA) estimations have been depicted in Fig 5. Measurement has been done by keeping the active-Tag at different positions with respect to a fixed position of the LBS (considered as the origin). The measurements are taken for the two different setups as mentioned in Table I.

In Fig 5, the blue coloured trace shows the path of the transmitted signal from the LBS while red coloured traces represent the paths of the received signals at the LBS. The sampling frequency of the data acquisition card has been kept at 22.5MHz, and the length of the baseline ($d_{baseline}$) is 0.30m. The '+/-δ'value corresponds to the difference in the AoA between the paths received on A1 and A2. Assuming that the distance between the LBS and the Tag is higher than $d_{baseline}$, the parallelism conditions are verified [5] and δ is found to be less significant.

To evaluate the performances of DMTD method, many positions of the active-Tag have been chosen inside [0.9 1.5m] for the range and [30° 90°] for the AoA. For performing measurements, we have assumed that the results for the AoA should be the same due to the symmetry of the LBS design. Therefore, the measurements are only done for a single quadrant for a sector of 60° (from 30° to 90°) (Fig 5). The theoretical 2D localization of the tag have been computed on MATLAB by taking into account only the wireless link between the LBS and the active-Tag by using the two frequency bandwidths (1GHz & 500MHz), respectively. Thereafter, the estimated positions obtained by the measurements are compared with the theoretical ones after subtracting the additional delays obtained by the calibration.

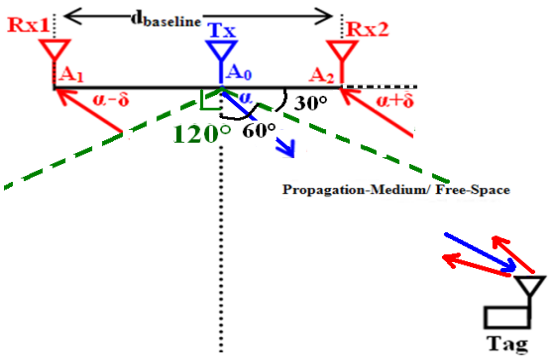


Fig. 5. Scheme for range & angle-of-arrival measurements

### D. Results

The Fig 6 shows an example of the baseband signals acquired for a given position of the active-Tag. The red and blue plots are the baseband signals collected by the data acquisition card from the FMCW signal with bandwidth equals to 1GHz and 500MHz, respectively.

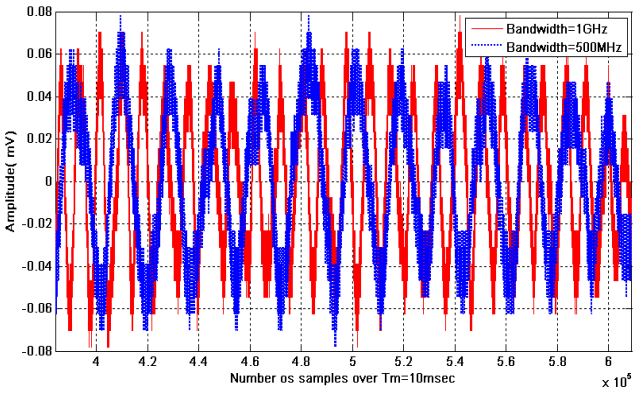


Fig. 6. Phase-shifts over swip time, Tm=10msec

This example shows the baseband signal acquired by a frequency bandwidth of 1GHz is relatively twice the frequency obtained by the bandwidth of 500MHz. Hence, the numbers of wavelengths acquired for 1GHz and 500MHz are 27 and 13 (Fig 6), respectively. Thus, the position of the remote active-Tag is estimated with N=27 and 13 (see relationships 5 and 6).

The performances of the system with 1GHz and 500MHz as frequency bandwidth are shown in Fig 7 & 8 in terms of error on the estimated ranges and angle-of-arrivals, respectively. The measurement covers the range [0.95 1.4 m] and the AoA inside [30° 90°].

In Fig 7, the errors in the estimated range given for the bandwidths of 1GHz and 500MHz are depicted in red and blue colours. The observed root-mean-square (*rms*) errors are shown in red and blue-dash lines which are equal to 6.5cm and 4.5cm, respectively. The values of the *rms* errors for the two bandwidths are closed that is a difference of 2 cm, only. The fluctuations on the two plots can be explained because of the harsh conditions of the considered indoor environment.

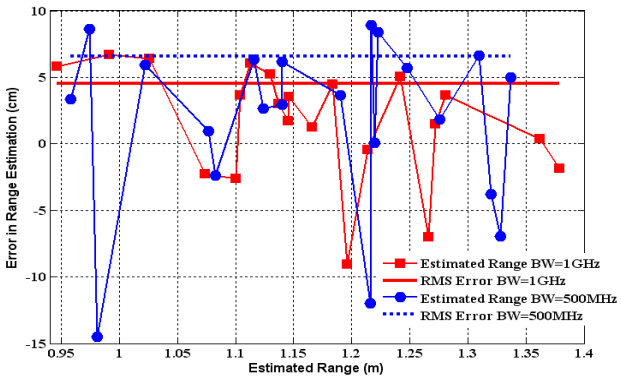


Fig. 7. Error on the measured range

The fluctuations on the error may be also due to a bad real active-Tag positioning in the investigated area as it becomes difficult to well mesh this area with an error lower than 1 cm. To estimate the real value on the active-Tag positioning, we are using a laser rangefinder.

In Fig 8, the error in AoA measurements are shown for the angles inside [30° 90°].

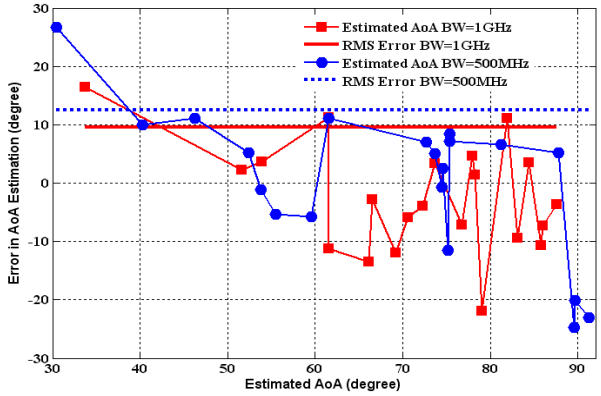


Fig. 8. Error on the measured AoA

The observed *rms* errors are 9.5° (red color) and 12.5°(blue color) for 1GHz and 500 MHz frenquency bandwidth, respectively. Only a differnece of 3° in the rms error is observed . The TABLE III summarizes the different values of the measured errors. The mean errors of range and AoA are also mentioned here.

TABLE III. RANGE AND AOA ERRORS

| **Parameter (error)** | **Bandwidth=1GHz** | | **Bandwidth=500MHz** | |
|---|---|---|---|---|
| | ***Range(cm)*** | ***AOA (degree)*** | ***Range(cm)*** | ***AOA (degree)*** |
| Abs. Mean | 3.9 | 7.9 | 5.5 | 9.9 |
| **Mean** | **1.6** | **-2.5** | **1.8** | **0.7** |
| *rms* | 4.5 | 9.5 | 6.5 | 12.5 |

The mean range error becomes 1.6 cm and 1.8 cm for the two studied frequency bandwidths. The mean AoA error becomes -2.5° and 0.7° respectively. These results aim that using a frequency bandwidth of 500 MHz with a DMDT method doesn't change the accuracy much compared to the results obtained with a frequency bandwidth of 1GHz and also of [5]. These values can be compared the results obtained by [3]. The observed mean values for range are quite close to each other and these values are almost ten times lesser than the values reported in [3]. The frequency bandwidth of 500 MHz was arbitrary chosen. Another study to know the optimum minimum value use of frequency bandwidth may be carried out; the current work only validate the concept that the use of lesser bandwidth (compared to 1GHz) can be undertaken without compromising much on the performance.

## IV. CONCLUSION

This paper shows the advantage of using a DMDT method jointly with the FMCW radar system for reducing the frequency bandwidth without any significant change in the accuracy of ranges and angle-of-arrivals for an indoor localization system. The performance has been done for 2D positioning in a real indoor environment in the line-of-sight case. This might be lead to a better spectrum management without damaging the localization in an indoor environment.

## *References*


[1] Yunchun Zhang; Zhiyi Fang; Ruixue Li; Wenpeng Hu; , "The Design and Implementation of a RSSI-Based Localization System," Wireless Communications, Networking and Mobile Computing, 2009.WiCom'09.5thInternational Conference on , vol., no.,pp.1-4,24-26 Sept.2009

[2] Narzullaev, A.; Yongwan Park; Hoyoul Jung; , "Accurate signal strength prediction based positioning for indoor WLAN systems," Position, Location and Navigation Symposium, 2008 IEEE/ION,vol.,no.,pp.685-688,5-8May2008,doi: 10.1109/PLANS.2008.4569989.

[3] R. H. Lee, C.C Chang, and S.F. Chang. , " A switched-beam FMCW radar for wireless indoor positioning system," European Radar conference, EuRAD, pp. 65-68, 2013.

[4] B. Waldmann, R. Weigel, R. Ebelt and M. Vossiek, " An ultra-wideband local positioning system for highly complex indoor environments," International Conference on Localization and GNSS, pp. 1-5, 2012.

[5] R. Kumar, J.C. Cousin, B. Huyart, and K. Mabrouk,"2D Measurement using interference and FMCW multistatic radar system for indoor localization," European Radar Conference, EuRAD, pp. 17-20, 2013.

[6] R. Barillet, J.Y. Richard, J. Cermak, and L. Sojdr, "Application of dual-mixer-time-differenc multiplication in accurate time-delay measurements," Frequency Control Symposium and Exposition, pp. 729-733, 2004.

[7] R. Kumar, J.C. Cousin, B. Huyart, and K. Mabrouk,"Antenne spirale asymétric couvrant la bande UWB [6-8.5 GHZ] pour une application de le localisation indoor," Jourées Nationales Microondes, French Conference, JNM, 2013.

[8] R. Kumar, J.C. Cousin, B. Huyart, and K. Mabrouk,"Dual-circular polarized dumbbell shaped crossed-dipole planar antenna for UWB application," European Antenna and Propagation, EuCAP, pp. 1474-1478, 2013.